Supporting Information

Corrosion-Resistant Microplasma Anode Array for High-Temperature Molten Salt Electrolysis and *In-Situ* Analysis

Junhan Luo [a], Qi Qing [a], Bo Liang [a], Shuang Liu [b], Zhe Wang [a,*], Jing Chen [a], Yuexiang Lu [a,*]

a. Institute of Nuclear and New Energy Technology, Tsinghua University, Beijing 100084, China.

b. Nuclear Research Institute for Future Technology and Policy, Seoul National University, Seoul 08826, Republic of Korea.

* Corresponding author: Zhe Wang, Email: wang2023@mail.tsinghua.edu.cn & Yuexiang Lu, E-mail: luyuexi-ang@mail.tsinghua.edu.cn

Product reduction degree calculation

The reduction degree was calculated by the air oxidation method using a thermogravimetric analyzer (TGA, Discovery STD650, TA Instruments). Before TGA measurement, the reduction products were crushed into small particles, a randomly selected approximately 20.0 mg sample, and loaded into an alumina crucible. The temperature was raised to 1273 K at a heating rate of 10 K/minute in an air atmosphere. Assuming that only U and unreduced UO_2 existed in the sample, the total sample mass before oxidation is given by **equation (1).**

$$n_U M_U + n_{UO_2} M_{UO_2} = m_1 \quad (1)$$

Where M_U(238.03 g·mol^{-1}) and M_{UO_2}(270.03 g·mol^{-1}) are the relative molecular mass of U and UO_2, n_U and n_{UO_2} are the molar amounts of U and UO_2, m_1 is the total sample mass before oxidation.

If the oxidation products were all U_3O_8, the total sample mass after oxidation can be express as **equation (2).**

$$\frac{M_{U_3O_8}}{3} n_U + \frac{M_{U_3O_8}}{3} n_{UO_2} = m_2 \quad (2)$$

Where $M_{U_3O_8}$(842.09 g·mol^{-1}) is the relative molecular mass of U_3O_8, m_2 is the total sample mass after oxidation.

The reduction degree η is defined as **equation (3)**.

$$\eta = \frac{n_U}{n_U + n_{UO_2}} \times 100\% \quad (3)$$

Substituting **equation (2)** into **equation (1)**, n_U and n_{UO_2} can be calculated as **equation (4) and equation (5).**

$$n_U = \frac{3M_{UO_2} m_2 - M_{U_3O_8} m_1}{M_{U_3O_8}(M_{UO_2} - M_U)} \quad (4)$$

$$n_{UO_2} = \frac{-3M_U m_2 + M_{U_3O_8} m_1}{M_{U_3O_8}(M_{UO_2} - M_U)} \quad (5)$$

Finally, inserting **equation (4) and equation (5)** into **equation (3)**, η can be expressed as **equation (6).**

$$\eta = \frac{3M_{UO_2} m_2 - M_{U_3O_8} m_1}{3(M_{UO_2} - M_U) m_2} = \frac{8.438 m_2 - 8.772 m_1}{m_2} \quad (6)$$

To analyze the concentrations of Cs^+ in the electrolyte, a quartz rod was inserted into the molten salt, and the cooled quenched salts were collected from the surface of the rod. Weighed the quenched salt and then dissolved it in 0.5M HNO_3. The concentrations of Cs^+ were tested by an inductively coupled plasma atomic emission spectrometer (ICP-AES, ARCOS FHS12, Spectro Scientific).

Fig. S1. Image of sintered UO_2 pellets wrapped with Mo wire before electrolysis.

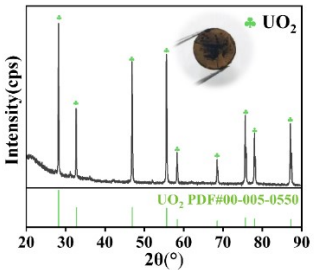

Fig. S2. XRD analysis and macroscopic morphology of the product, which used the UO_2 pellet un-sintered as the cathode.

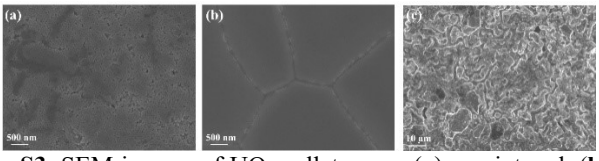

Fig. S3. SEM images of UO_2 pellets were (**a**) un-sintered, (**b**)

sintered at 1773 K, and **c** reduction product (sintered at 1773 K).

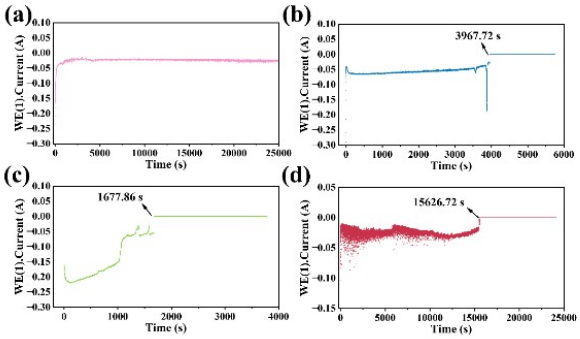

Fig. S4. Current-time plots of electrolysis by using the (**a**) carbon anode, (**b**) Pt anode, (**c**) Mo anode, and (**d**) W anode in LiCl melt.

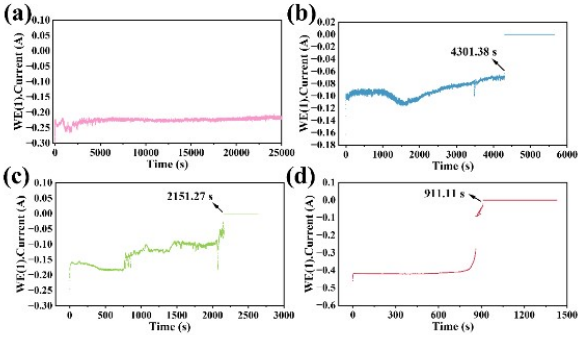

Fig. S5. Current-time plots of electrolysis by using the (**a**) carbon anode, (**b**) Pt anode, (**c**) Mo anode, and (**d**) W anode in LiCl-Li_2O melt.

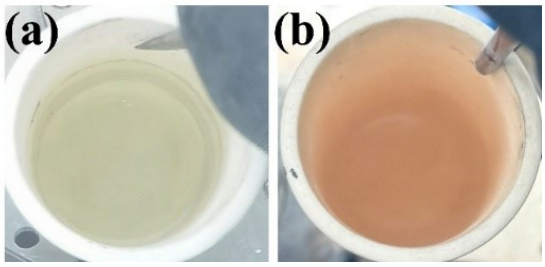

Fig. S6. Images of (**a**) LiCl and (**b**) LiCl-Li_2O molten salt before electrolysis.

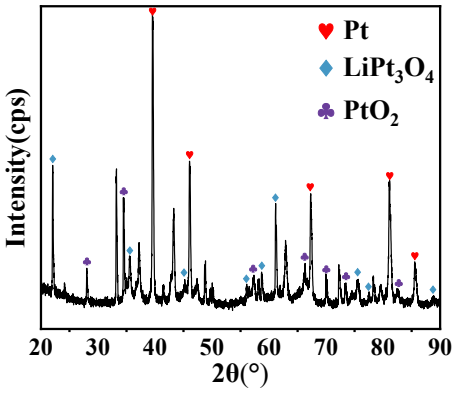

Fig. S7. XRD analysis of the surface product of the Pt anode.

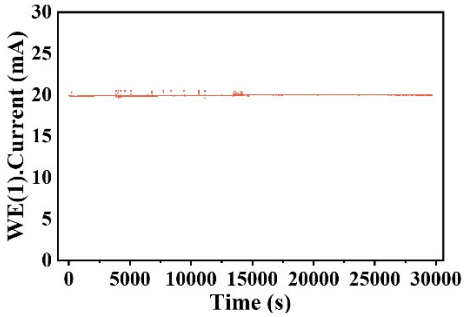

Fig. S8. Current-time plots of electrolysis by using the microplasma anode.

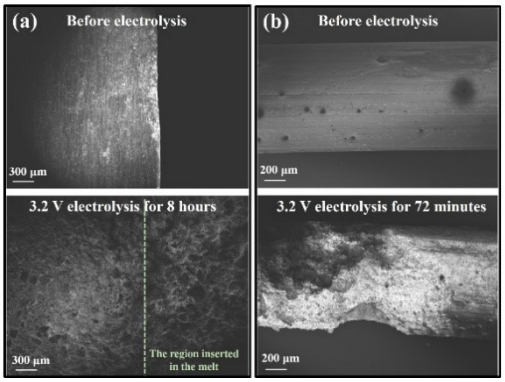

Fig. S9. The morphology image of the (**a**) carbon anode, and (**b**) Pt anode before and after electrolysis in LiCl-Li_2O molten salts.

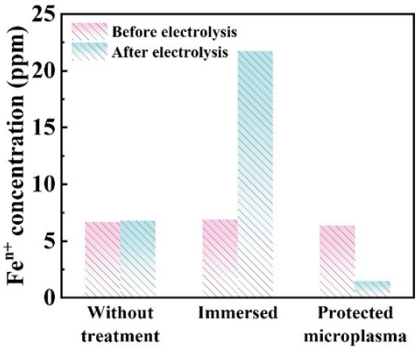

Fig. S10. The Fe^{n+} ions concentration changes in the melt after different electrolysis treatments.

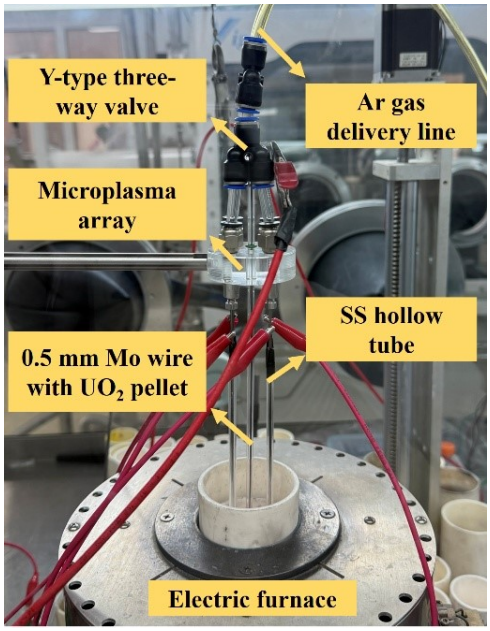

Fig. S11. The photograph of a microplasma array with four microplasmas used in molten salt.